9737Rb60: The cornerstone of the region of deformation around A 100

Sotty, C.; Zielinska, M.; Georgiev, G.; Balabanski, D. L.; Stuchbery, A. E.; Blazhev, A.; Bree, N.; Chevrier, R.; Das Gupta, S.; Daugas, J. M.; Davinson, T.; De Witte, H.; Diriken, J.; Gaffney, L. P.; Geibel, K.; Hadynska-Klek, K.; Kondev, F. G.; Konki, J.; Kroell, T.; Morel, P.; Napiorkowski, P.; Pakarinen, J.; Reiter, P.; Scheck, M.; Seidlitz, M.; Siebeck, B.; Toernqvist, H.; Warr, N.; Wenander, F.

Published in:
Physical Review Letters

DOI:
10.1103/PhysRevLett.115.172501
10.1103/PhysRevLett.115.209902

Published: 23/10/2015

Document Version
Publisher's PDF, also known as Version of record

$^{97}_{37}Rb_{60}$: The Cornerstone of the Region of Deformation around $A \sim 100$

C. Sotty,[1,2] M. Zielińska,[3,4] G. Georgiev,[1,*] D. L. Balabanski,[5] A. E. Stuchbery,[6] A. Blazhev,[7] N. Bree,[2] R. Chevrier,[8] S. Das Gupta,[9,†] J. M. Daugas,[8] T. Davinson,[10] H. De Witte,[2] J. Diriken,[2,11] L. P. Gaffney,[12,2,‡] K. Geibel,[7] K. Hadyńska-Klęk,[3] F. G. Kondev,[13] J. Konki,[14,15,16] T. Kröll,[17] P. Morel,[8] P. Napiorkowski,[3] J. Pakarinen,[14,15,16] P. Reiter,[7] M. Scheck,[17,‡] M. Seidlitz,[7] B. Siebeck,[7] G. Simpson,[18] H. Törnqvist,[14] N. Warr,[7] and F. Wenander[14]

[1]*CSNSM, CNRS/IN2P3, Université Paris-Sud, UMR8609, F-91405 ORSAY-Campus, France*
[2]*KU Leuven, Instituut voor Kern- en Stralingsfysica, 3001 Leuven, Belgium*
[3]*Heavy Ion Laboratory, University of Warsaw, 02-093 Warsaw, Poland*
[4]*IRFU/SPhN, CEA Saclay, F-91191 Gif-sur-Yvette, France*
[5]*ELI-NP, IFIN-HH, 30 Reactorului Street, 077125 Bucharest, Măgurele, Romania*
[6]*Department of Nuclear Physics, RSPE, Australian National University, Canberra, Australian Capital Territory 2601, Australia*
[7]*Institute for Nuclear Physics, University of Cologne, Zülpicher Straße 77, D-50937 Cologne, Germany*
[8]*CEA, DAM, DIF, F-91297 Arpajon cedex, France*
[9]*Dipartimento di Fisica, Universitá di Camerino, I-62032 Camerino, Italy and Istituto Nazionale di Fisica Nucleare, Sezione di Perugia, I-06123 Perugia, Italy*
[10]*Department of Physics and Astronomy, University of Edinburgh, Edinburgh EH9 3JZ, United Kingdom*
[11]*Belgian Nuclear Research Centre SCK·CEN, Boeretang 200, B-2400 Mol, Belgium*
[12]*Oliver Lodge Laboratory, University of Liverpool, Liverpool L69 7ZE, United Kingdom*
[13]*Nuclear Engineering Division, Argonne National Laboratory, Argonne, Illinois 60439, USA*
[14]*ISOLDE, CERN, CH-1211 Geneva 23, Switzerland*
[15]*Department of Physics, University of Jyväskylä, P.O. Box 35, FI-40014 University of Jyväskylä, Finland*
[16]*Helsinki Institute of Physics, University of Helsinki, P.O. Box 64, FI-00014 Helsinki, Finland*
[17]*Institut für Kernphysik, Technische Universität Darmstadt, D-64289 Darmstadt, Germany*
[18]*LPSC, CNRS/IN2P3, Université Joseph Fourier Grenoble 1, CNRS/IN2P3, INPG, F-38026 Grenoble Cedex, France*

(Received 3 August 2015; published 20 October 2015; publisher error corrected 5 November 2015)

Excited states of the neutron-rich nuclei ^{97,99}Rb were populated for the first time using the multistep Coulomb excitation of radioactive beams. Comparisons of the results with particle-rotor model calculations provide clear identification for the ground-state rotational band of ^{97}Rb as being built on the $\pi g_{9/2}[431]\,3/2^+$ Nilsson-model configuration. The ground-state excitation spectra of the Rb isotopes show a marked distinction between single-particle-like structures below $N = 60$ and rotational bands above. The present study defines the limits of the deformed region around $A \sim 100$ and indicates that the deformation of ^{97}Rb is essentially the same as that observed well inside the deformed region. It further highlights the power of the Coulomb-excitation technique for obtaining spectroscopic information far from stability. The ^{99}Rb case demonstrates the challenges of studies with very short-lived postaccelerated radioactive beams.

DOI: 10.1103/PhysRevLett.115.172501 PACS numbers: 27.60.+j, 23.20.Lv, 25.70.De, 29.38.-c

The spherical symmetry of atomic nuclei is well established for the cases where both the proton (Z) and neutron (N) numbers are near magic numbers. Most atomic nuclei, however, have nonspherical shapes. The best-known and well-studied region of prolate-deformed nuclei is the "rare-earth region," centered between $50 < Z < 82$ and $82 < N < 126$. A less known region of deformed nuclei, which is predicted to show even larger deformations [1], is centered around mass 100 ($A \sim 100$) between the $28 < Z < 50$ and $50 < N < 82$ major shells. These nuclei are neutron rich, and well away from the valley of stability, so they are challenging to study experimentally.

The $A \sim 100$ prolate-deformed Sr-Zr region ($Z = 38, 40$) has attracted considerable attention since its prediction [2] and experimental observation [3]. Spectroscopic studies of these neutron-rich nuclei were undertaken at on-line mass separators and by γ-ray spectroscopy in spontaneous fission [4–6]. A key feature is the sudden onset of deformation when progressing from neutron number $N = 58$ to $N = 60$. However, the abrupt change of the deformation quickly washes out when moving away from $Z = 38$ [4].

Nuclei at the border of this deformed region, in which the addition or the removal of a single nucleon results in a large shape change, hold the key to its understanding. Tracking

the shape changes in the odd-neutron nuclei has shown that the $\nu g_{7/2}$ orbit plays a crucial role. A number of rotational bands, based on Nilsson orbits with $\nu g_{7/2}$ parentage, have been observed in the odd-A Sr and Zr nuclei (see Ref. [6] and references therein).

The evolution of the deformation as a function of the proton number is not so well studied. Ground-state rotational bands in the odd-A $_{39}$Y nuclei are suggested to be built on the $\pi g_{9/2}\,[422]\,5/2^+$ Nilsson state [7]. However, the onset of deformation in the $_{37}$Rb isotopes is less understood. Ground-state spin and moment studies of the Rb isotopes [8] revealed a sudden onset of deformation in $^{97}\mathrm{Rb}_{60}$ but failed to clearly identify whether it is associated with the $\pi g_{9/2}[431]3/2^+$ or the $\pi p_{3/2}[301]3/2^-$ Nilsson orbital. Mean-square-charge radii [9] and two-neutron separation energies [10] confirmed the *sudden* structural change at $N = 60$ in the Rb nuclei. In contrast, mean-square-charge radii [9], mass measurements [11], and Coulomb-excitation [12] studies demonstrated that deformation in the Kr ($Z = 36$) isotopes develops *smoothly* across $N = 60$.

In this Letter we report Coulomb-excitation measurements on the neutron-rich isotopes $^{97}\mathrm{Rb}_{60}$ and $^{99}\mathrm{Rb}_{62}$ produced as radioactive beams. The excited states in these odd-A nuclei at the border of the $A \sim 100$ deformed region were observed for the first time, finding that they form rotational bands built on the ground state. The results provide clear-cut evidence for enhanced quadrupole collectivity of the ^{97,99}Rb nuclei and firmly identify the deformation-driving configuration of the odd proton. They also establish the limits both in N and Z (cornerstone) of the region of deformed nuclei around $A \sim 100$. Prior to the present experiment, the experimental information on Rb isotopes at and beyond $N = 60$ was limited to ground-state properties and no excited states were known. An excited rotational band was observed in $^{96}\mathrm{Rb}_{59}$ [13] providing evidence for shape coexistence in that nucleus. During the data analysis of the present work an isomeric $E1$ transition in ^{97}Rb was reported [14,15].

The experiment was performed at the REX-ISOLDE facility [16] at CERN. The species of interest were produced by a 1.4 GeV proton beam on a UC_x target. They were surface ionized and mass separated through the High Resolution Separator (HRS) before being sent to the REX-TRAP [17] for bunching and charge breeding in REX-EBIS [18]. The short half-lives of ^{97}Rb [$T_{1/2} = 169.1(6)$ ms] and ^{99}Rb [$T_{1/2} = 54(4)$ ms] required short trapping and breeding times [82 (70) and 69 ms (69 ms), respectively, for ^{97}Rb (^{99}Rb)] in order to minimize in-flight decay. The beam was postaccelerated to 2.85(3) MeV/u by the REX-LINAC [19], delivering average beam intensities for ^{97}Rb and ^{99}Rb of 5×10^5 pps and a few times 10^3 pps, respectively. A 2.1 mg/cm^2 ^{60}Ni target was used to Coulomb excite the nuclei of interest. The experimental

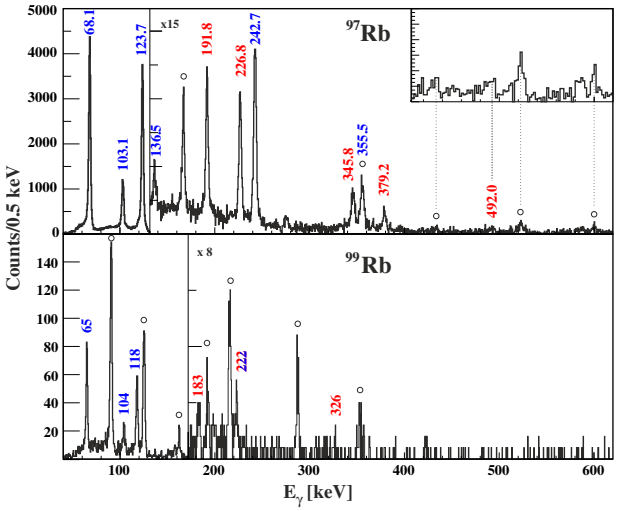

FIG. 1 (color online). Doppler corrected γ-ray energy spectra for ^{97}Rb (upper panel) and ^{99}Rb (lower panel). Transitions, identified as belonging to Rb isotopes, are marked with their energies. Contaminating transitions, from the Coulomb excitation of Sr isotopes, are marked with circles.

setup consisted of the Miniball γ-ray spectrometer [20] coupled to a double-sided silicon strip detector [21]. The γ rays depopulating the excited states were measured in coincidence with target nuclei scattered into the double-sided silicon strip detector. To avoid unsafe Coulomb excitation [22], the particle detection was limited to the center-of-mass angular range of 74°–113°. Examples of the γ-ray spectra are presented in Fig. 1.

γ-γ coincidence matrices were constructed to establish the level schemes of ^{97}Rb and ^{99}Rb shown in Fig. 2. The γ-ray intensities (see Tables I and II and Fig. 1) were obtained using singles spectra except for the 355.5-keV transition in ^{97}Rb and the two 222-keV transitions in ^{99}Rb. The 355.5-keV transition was contaminated by the 355.3-keV transition in ^{97}Sr, also populated in Coulomb excitation. Because of the low statistics, the two 222-keV transitions in ^{99}Rb could not be separated and the total intensity is given in Table II.

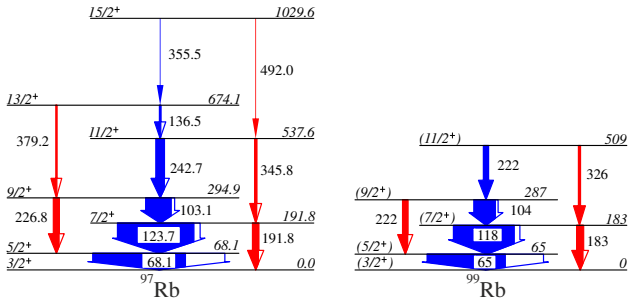

FIG. 2 (color online). Level schemes for ^{97}Rb and ^{99}Rb as obtained in the present experiment. Pure $E2$ transition are marked in red while mixed ($M1/E2$) are in blue.

TABLE I. Intensities for γ-ray transitions observed in ^{97}Rb and corresponding $B(E2)$ and $B(M1)$ transition probabilities. No transition probabilities could be determined for the 68-keV transition because of the unknown $E2/M1$ mixing ratio.

E_x (keV)	I_i^π	I_f^π	E_γ (keV)	$I_\gamma \times 10^3$	$B(E2)$ $[e^2b^2]$	$B(M1)$ $[\mu_N^2]$
68.1	$5/2^+$	$3/2^+$	68.1	114(34)		
191.8	$7/2^+$	$3/2^+$	191.8	4.96(19)	0.22^{+8}_{-10}	
191.8	$7/2^+$	$5/2^+$	123.7	67(2)	0.33^{+11}_{-14}	0.28^{+11}_{-12}
294.9	$9/2^+$	$5/2^+$	226.8	4.47(19)	0.18^{+4}_{-2}	
294.9	$9/2^+$	$7/2^+$	103.1	18.68(36)	0.12^{+2}_{-1}	0.29^{+6}_{-4}
537.6	$11/2^+$	$7/2^+$	345.8	2.99(16)	0.24^{+4}_{-5}	
537.6	$11/2^+$	$9/2^+$	242.7	7.48(23)	0.093^{+14}_{-20}	0.15^{+3}_{-3}
674.1	$13/2^+$	$9/2^+$	379.2	1.61(14)	0.22^{+3}_{-2}	
674.1	$13/2^+$	$11/2^+$	136.5	0.98(17)	0.056^{+6}_{-5}	0.28^{+6}_{-5}
1029.6	$15/2^+$	$11/2^+$	492.0	0.39(7)	0.28^{+4}_{-4}	
1029.6	$15/2^+$	$13/2^+$	355.5	0.64(11)	0.052^{+7}_{-8}	0.20^{+7}_{-5}

The beam composition was evaluated by the ΔE-E technique using an ionization chamber (ΔE) and a Si (E) detector. The beam composition for the mass 97 beam was 74(6)% ^{97}Rb, 19(6)% ^{97}Sr, and 7(1)% ^{97}Y. The entire Y contribution and the predominant part of the Sr contribution were due to the in-flight decay of ^{97}Rb during the ~150 ms trapping and breeding of the ions. The beam composition for the mass 99 case [85(3)% ^{86}Kr, 6(2)% ^{99}Rb, 7(2)% ^{99}Sr, and 2(1)% ^{99}Y] showed considerable ^{86}Kr contamination from EBIS residual gas due to a very similar mass-over-charge ratio to the ^{99}Rb beam. The much worse ^{99}Rb-to-^{99}Sr ratio was a result of the relatively long trapping and breeding times (~140 ms) compared to the half-life of ^{99}Rb. This shows that lifetimes of the order of 50 ms are about the limit of applicability for postaccelerated Isotope Separator OnLine (ISOL) beam techniques.

Matrix elements were extracted from the measured transition intensities using the code GOSIA [23]. For the six strongest transitions the data were divided into three subsets corresponding to three different ranges of center-of-mass scattering angles (74°–83°, 83°–99°, 99°–113°) in order to exploit the angular dependence of the excitation probability. Sixteen $E2$ and six $M1$ matrix elements, coupling the seven observed states, were fitted to the 23 measured γ-ray intensities.

TABLE II. Intensities for γ-ray transitions observed in ^{99}Rb.

E_x (keV)	I_i^π	I_f^π	E_γ (keV)	I_γ[a]
65	$(5/2^+)$	$(3/2^+)$	65	1640(100)
183	$(7/2^+)$	$(3/2^+)$	183	90(20)
183	$(7/2^+)$	$(5/2^+)$	118	970(60)
287	$(9/2^+)$	$(5/2^+)$	222	170(80)*
287	$(9/2^+)$	$(7/2^+)$	104	230(110)
509	$(11/2^+)$	$(7/2^+)$	326	50(17)
509	$(11/2^+)$	$(9/2^+)$	222	170(80)*

[a]Total intensity given for the unresolved 222 keV doublet.

The Coulomb excitation of a specific state is governed mostly by $E2$ matrix elements. However, the decay intensities, which are the actual experimental observables, may be strongly influenced by the $M1$ matrix elements. The $E2$ excitation probabilities cannot be unambiguously determined without additional constraints on $M1$ matrix elements. As neither lifetimes nor mixing ratios are available, a model-dependent approach was used. In the ^{97}Rb case it was assumed that $E2$ transitions deexciting each state follow the Alaga rules [24] and therefore the ratio of their matrix elements ($\langle J\|E2\|J-1\rangle/\langle J\|E2\|J-2\rangle$) depends only on a geometrical factor (Clebsch-Gordan coefficients). This assumption can be justified first by noting that all observed states form a rotational band, and second, that all observations are consistent with particle-rotor model calculations, as discussed below.

In the first stage of the analysis the $\langle 7/2^+\|E2\|3/2^+\rangle$ matrix element in ^{97}Rb was determined relative to the observed excitation of the target nucleus ^{60}Ni. This procedure used the observed γ-ray intensities in ^{97}Rb and ^{60}Ni, as well as known spectroscopic data for the latter [$B(E2)$ and the quadrupole moment [25]]. In the fit, all matrix elements in ^{97}Rb were allowed to vary with only the constraints from the Alaga rules. Corrections for the beam composition were taken into account. In the second step of the analysis the remaining matrix elements were obtained relative to $\langle 7/2^+\|E2\|3/2^+\rangle$.

A similar analysis of the ^{99}Rb data was not possible due to the much lower statistics, nonobservation of target excitation, and the presence of an unresolved doublet at 222 keV. A more model-dependent approach was adopted, with all $E2$ matrix elements in ^{99}Rb coupled assuming the rotational model, i.e., $\langle I_f\|E2\|I_i\rangle = \sqrt{2I_i+1}(I_i,K,2,0|I_f,K)\sqrt{\frac{5}{16}}eQ_0$, where $(I_i,K,2,0|I_f,K)$ is a Clebsch-Gordan coefficient, and Q_0 is the transitional quadrupole moment, directly related to the nuclear deformation. Only a single Q_0 and four $M1$ matrix elements were fitted to the entire band. The value $Q_0 = 2.8^{+0.4}_{-0.6}$ eb was obtained. This approach has been validated using the ^{97}Rb data, which yielded a $Q_0(^{97}\mathrm{Rb})$ value (see Fig. 3) consistent with the weighted mean value from the individual $Q_0(J)$.

Figure 3 compares the transitional quadrupole moments Q_0 for individual levels in ^{97}Rb to experimental values for Zr, Sr, and Kr isotones at $N = 58$–62. The deformation of the ground-state band in ^{97}Rb obtained from the present experiment is in agreement with the result of the earlier laser-spectroscopy measurement of the ground-state spectroscopic quadrupole moment [8]. The Q_0 values obtained for ^{97}Rb remain remarkably constant within the

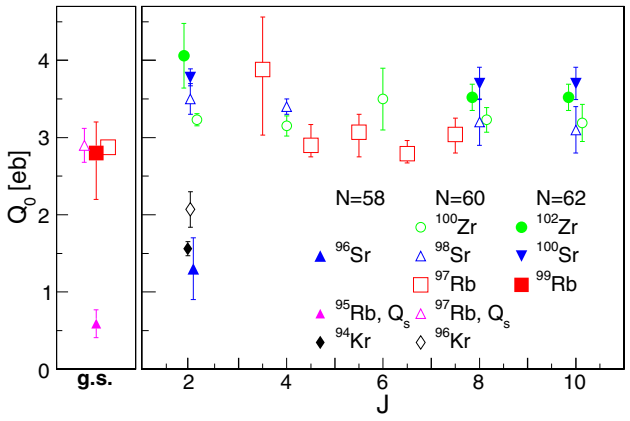

FIG. 3 (color online). Transitional quadrupole moments, Q_0, for the even-even Kr, Sr, Zr [12,25–29] and the odd-mass Rb isotopes (present measurement) as a function of spin. The values for the ground states of ^{95,97,99}Rb (left side) were obtained either from the analysis of the present data (squares), under the assumption of the rotational model, or from spectroscopic quadrupole moments (triangles) [8]. The values for the excited states were calculated from measured transition probabilities. Some of the values for the even-even cases are slightly displaced on the x axis for clarity.

band and similar in magnitude to those observed for $N = 60, 62$ Zr and Sr isotopes. Within experimental uncertainties there is no change in the deformation between ^{97}Rb and ^{99}Rb, similar to what is observed in the Sr and Zr isotopes. The sudden onset of ground-state deformation at $N = 60$, as a function of the proton number, starts only from the Rb isotopes. Thus, (i) ^{97}Rb is the southwest border of the well-deformed $A \sim 100$ region, and (ii) although right at the border, the deformation of ^{97}Rb is essentially the same as that observed inside the deformed region.

Particle-rotor model calculations based on a standard Woods-Saxon potential [30] were performed to shed light on the structure of the ground-state band of ^{97}Rb. A Nilsson diagram is shown in Fig. 4. Particular attention was given to the $B(M1)/B(E2)$ ratios shown in the upper panel of Fig. 5, which were determined solely from γ-ray energies and branching ratios (see, e.g., [32]). Calculations were performed for both positive and negative parity states because the measured magnetic moment of the ground state suggests, but does not distinguish between, the Nilsson orbits $[431]3/2^+$ and $[301]3/2^-$. The quadrupole deformation parameter was set to $\beta_2 = 0.31$, consistent with the average of the measured Q_0 values. The hexadecapole deformation was varied between $\beta_4 = 0$ and $\beta_4 = 0.06$, the latter value being that predicted by Möller *et al.* [33]. The level energies, ground-state moments, and $E2$ transition strengths were described equally well for either a $[431]3/2^+$ or a $[301]3/2^-$ band. The lower panel of Fig. 5 compares $B(E2)$ calculations for the $[431]3/2^+$ band with experimental values obtained from the GOSIA analysis. These comparisons justify the

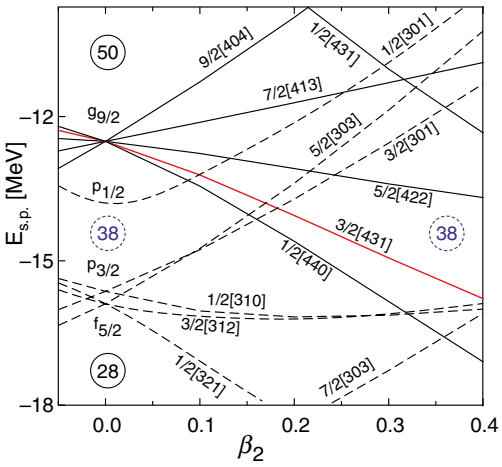

FIG. 4 (color online). Nilsson diagram for protons in the $A \sim 100$ region. The single-particle energies are calculated using the Woods-Saxon model with the "universal parametrization" and $\beta_4 = \beta_2^2/6$ and $\beta_6 = 0$, where β_2, β_4, and β_6 are deformation parameters [31].

use of the Alaga rules to constrain the fit during the data analysis.

The $M1$ transition strengths for $[431]3/2^+$ and $[301]3/2^-$ bands are also quite similar in magnitude because the two bands have similar intrinsic g factors (g_K values). Nevertheless, the $B(M1)/B(E2)$ ratios in the upper panel of Fig. 5 rule out the $[301]3/2^-$ candidate. Coriolis mixing between the $K = 3/2$ ground-state band and adjacent $K = 1/2$ bands causes the $M1$ transitions to show a sawtoothlike signature dependence. The Coriolis-mixed wave functions show that mixing between the $[431]3/2^+$ and $[440]1/2^+$ bands is responsible for the

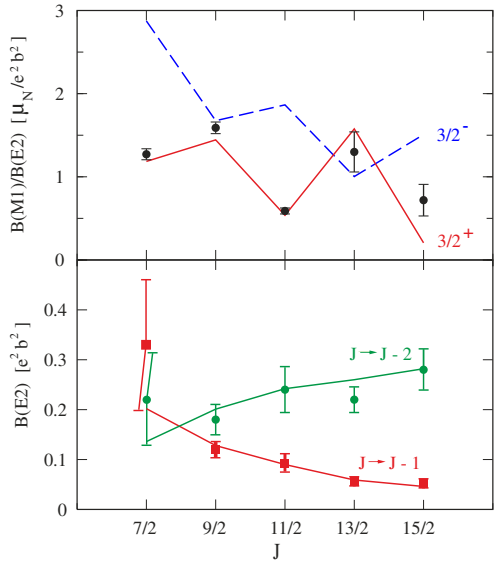

FIG. 5 (color online). Particle-rotor model calculations for ^{97}Rb compared with experiment. Upper panel: $B(M1)/(E2)$ ratios. Lower panel: $B(E2)$ values. See text for more details.

observed dip in the $M1$ strength of the $11/2^+ \rightarrow 9/2^+$ transition, seen in the upper panel of Fig. 5. There are two properties of the $[440]1/2^+$ band that lead to the observed pattern. The first is that the magnetic decoupling parameter is negative, $b_0 \simeq -3$, which produces a saw-tooth pattern in phase with the data. The second is that the energy decoupling parameter $a \simeq 4.5$ is large, thus, pushing down the $K = 1/2$ states with spin $J^\pi = 1/2^+, 5/2^+, 9/2^+, \ldots$, to mix strongly with the $K = 3/2$ ground-state band, while the $K = 1/2$ states with spin $J^\pi = 3/2^+, 7/2^+, 11/2^+, \ldots$, are pushed up in energy and hardly mix with the ground-band levels. Coriolis mixing of the $9/2^+$ states causes the reduced $B(M1; 11/2^+ \rightarrow 9/2^+)$ transition rate.

The negative parity alternative, mixing of the $[310]1/2^-$ band with the $[301]3/2^-$ band, cannot explain the data. It predicts the wrong signature dependence of the $M1$ transitions because $b_0 \simeq +1$.

Thus, the observed trends in the $M1$ transition rates and $B(M1)/B(E2)$ ratios confirm the $\pi g_{9/2}$ $[431]3/2^+$ Nilsson configuration for the ground-state band of ^{97}Rb. This assignment is in agreement with the conclusions of a recent theoretical study of odd-A Rb isotopes [34]. The isomeric $E1$ transition that has since been identified in ^{97}Rb probably originates from a negative parity Nilsson configuration [14,15].

The sudden onset of deformation at $N = 60$ in the Rb isotopes suggests a tip of the balance from the spherical shell gap at $Z = 38$ for $N \leq 58$ to the deformed shell gap at $Z = 38$ for $N = 60, 62$. The spherical and deformed shell gaps at $Z = 38$ are indicated in Fig. 4. Deformed shell gaps near $\beta_2 = 0.3$ also occur for neutrons at $N = 60$ and $N = 62$. Thus, the deformed shell gaps for both protons and neutrons evidentally play an important role in the sudden onset of deformation and its near constant value once established [6].

In summary, the first identification of excited states in the neutron-rich nuclei ^{97,99}Rb was achieved by multistep Coulomb excitation of these odd-mass radioactive beams. The level schemes and transition probabilities were determined in the ground-state rotational bands. Detailed information on the $M1$ transition strengths in ^{97}Rb provided clear-cut experimental evidence for the $\pi g_{9/2}$ $[431]3/2^+$ Nilsson-configuration assignment. The results define the "southwest" corner of the region of deformation around $A \sim 100$.

This work was supported by the European Union Seventh Framework through ENSAR (Contract No. 262010), and the German BMBF under Contracts No. 06KY9136I, No. 05P12PKFNE, No. 05P15PKCIA, No. 06DA9036I, No. 05P12RDCIA, and No. 05P15RDCIA. Work at ANL is supported by the U.S. Department of Energy, Office of Science, Office of Nuclear Physics under Contract No. DE-AC02-06CH11357.

*Corresponding author.
Georgi.Georgiev@csnsm.in2p3.fr
†Present address: Department of Physics, Heritage Institute of Technology, Kolkata 700107, India.
‡University of the West of Scotland, Paisley PA1 2BE, United Kingdom and SUPA, Scottish Universities Physics Alliance, Glasgow G12 8QQ, United Kingdom.

[1] P. Möller and J. R. Nix, At. Data Nucl. Data Tables **26**, 165 (1981).
[2] D. Arseniev, A. Sobiczewski, and V. Soloviev, Nucl. Phys. **A139**, 269 (1969).
[3] E. Cheifetz, R. C. Jared, S. G. Thompson, and J. B. Wilhelmy, Phys. Rev. Lett. **25**, 38 (1970).
[4] J. Hamilton, *Structures of Nuclei Far From Stability*, Treatise on Heavy Ion Science, Vol. 8 (Plenum Press, New York, 1989), pp. 2–98.
[5] I. Ahmad and W. Phillips, Rep. Prog. Phys. **58**, 1415 (1995).
[6] J. Hamilton, A. Ramayya, S. Zhu, G. Ter-Akopian, Y. Oganessian, J. Cole, J. Rasmussen, and M. Stoyer, Prog. Part. Nucl. Phys. **35**, 635 (1995).
[7] F. K. Wohn, J. C. Hill, R. F. Petry, H. Dejbakhsh, Z. Berant, and R. L. Gill, Phys. Rev. Lett. **51**, 873 (1983).
[8] C. Thibault, F. Touchard, S. Büttgenbach, R. Klapisch, M. de Saint Simon, H. T. Duong, P. Jacquinot, P. Juncar, S. Liberman, P. Pillet *et al.*, Phys. Rev. C **23**, 2720 (1981).
[9] M. Keim, E. Arnold, W. Borchers, U. Georg, A. Klein, R. Neugart, L. Vermeeren, R. Silverans, and P. Lievens, Nucl. Phys. **A586**, 219 (1995).
[10] J. Hakala, R. Rodríguez-Guzmán, V.-V. Elomaa, T. Eronen, A. Jokinen, V. Kolhinen, I. Moore, H. Penttilä, M. Reponen, J. Rissanen *et al.*, Eur. Phys. J. A **47**, 129 (2011).
[11] S. Naimi, G. Audi, D. Beck, K. Blaum, C. Böhm, C. Borgmann, M. Breitenfeldt, S. George, F. Herfurth, A. Herlert *et al.*, Phys. Rev. Lett. **105**, 032502 (2010).
[12] M. Albers, N. Warr, K. Nomura, A. Blazhev, J. Jolie, D. Mücher, B. Bastin, C. Bauer, C. Bernards, L. Bettermann *et al.*, Phys. Rev. Lett. **108**, 062701 (2012).
[13] J. A. Pinston, J. Genevey, R. Orlandi, A. Scherillo, G. S. Simpson, I. Tsekhanovich, W. Urban, H. Faust, and N. Warr, Phys. Rev. C **71**, 064327 (2005).
[14] D. Kameda, T. Kubo, T. Ohnishi, K. Kusaka, A. Yoshida, K. Yoshida, M. Ohtake, N. Fukuda, H. Takeda, K. Tanaka *et al.*, Phys. Rev. C **86**, 054319 (2012).
[15] M. Rudigier, G. S. Simpson, J. M. Daugas, A. Blazhev, C. Fransen, G. Gey, M. Hackstein, J. Jolie, U. Köster, T. Malkiewicz *et al.*, Phys. Rev. C **87**, 064317 (2013).
[16] D. Habs, O. Kester, G. Bollen, L. Liljeby, K. Rensfelt, D. Schwalm, R. von Hahn, G. Walter, and P. V. Duppen, Nucl. Phys. **A616**, 29 (1997).
[17] F. Ames, G. Bollen, P. Delahaye, O. Forstner, G. Huber, O. Kester, K. Reisinger, and P. Schmidt, Nucl. Instrum. Methods Phys. Res., Sect. A **538**, 17 (2005).
[18] F. Wenander, J. Instrum. **5**, C10004 (2010).
[19] D. Voulot, F. Wenander, E. Piselli, R. Scrivens, M. Lindroos, H. Jeppesen, L. Fraile, S. Sturm, and P. Delahaye, Nucl. Instrum. Methods Phys. Res., Sect. B **266**, 4103 (2008).
[20] N. Warr, J. Van de Walle, M. Albers, F. Ames, B. Bastin, C. Bauer, V. Bildstein, A. Blazhev, S. Bönig, N. Bree *et al.*, Eur. Phys. J. A **49**, 40 (2013).

[21] A. Ostrowski, S. Cherubini, T. Davinson, D. Groombridge, A. Laird, A. Musumarra, A. Ninane, A. di Pietro, A. Shotter, and P. Woods, Nucl. Instrum. Methods Phys. Res., Sect. A **480**, 448 (2002).
[22] D. Cline, Annu. Rev. Nucl. Part. Sci. **36**, 683 (1986).
[23] T. Czosnyka, D. Cline, and C. Wu, Bull. Am. Phys. Soc. **28**, 745 (1983).
[24] G. Alaga, K. Alder, A. Bohr, and B. Mottelson, Dan. Mat. Fys. Medd. **29**, 1 (1955).
[25] S. Raman, C. N. Nestor Jr., and P. Tikkanen, At. Data Nucl. Data Tables **78**, 1 (2001).
[26] H. Mach, F. Wohn, G. Molnár, K. Sistemich, J. C. Hill, M. Moszyński, R. Gill, W. Krips, and D. Brenner, Nucl. Phys. **A523**, 197 (1991).
[27] H. Mach, M. Moszyński, R. Gill, F. Wohn, J. Winger, J. C. Hill, G. Molnár, and K. Sistemich, Phys. Lett. B **230**, 21 (1989).
[28] A. G. Smith, R. M. Wall, D. Patel, G. S. Simpson, D. M. Cullen, J. L. Durell, S. J. Freeman, J. C. Lisle, J. F. Smith, B. J. Varley *et al.*, J. Phys. G **28**, 2307 (2002).
[29] A. G. Smith, J. L. Durell, W. R. Phillips, W. Urban, P. Sarriguren, and I. Ahmad, Phys. Rev. C **86**, 014321 (2012).
[30] P. Semmes and I. Ragnarson, The Particle+Triaxial Rotor Model: A User's Guide (unpublished), distributed at the Hands-On Nuclear Theory Workshop, Oak Ridge, August 5–16, 1991.
[31] S. Cwiok, J. Dudek, W. Nazarewicz, J. Skalski, and T. Werner, Comput. Phys. Commun. **46**, 379 (1987).
[32] A. Bohr and B. R. Mottelson, *Nuclear Structure* (W.A. Benjamin, Inc., London, 1975).
[33] P. Möller, J. Nix, W. Myers, and W. Swiatecki, At. Data Nucl. Data Tables **59**, 185 (1995).
[34] R. Rodriguez-Guzman, P. Sarriguren, and L. M. Robledo, Phys. Rev. C **82**, 061302 (2010).